

Au^I-Catalyzed Hydroalkynylation of Haloalkynes

Pedro D. García-Fernández,[†] Javier Iglesias-Sigüenza,[†] Paula S. Rivero-Jerez,^{†,∇} Elena Díez,^{*,†} Enrique Gómez-Bengoa,^{*,‡} Rosario Fernández,^{*,†} and José M. Lassaletta^{*,§}

[†] Departamento de Química Orgánica (Universidad de Sevilla) and Centro de Innovación en Química Avanzada (ORFEO-CINQA), C/ Prof. García González 1, 41012 Sevilla, Spain, E-mail: ffernan@us.es

[‡] Departamento de Química Orgánica I, Universidad del País Vasco, UPV/EHU, Apdo. 1072, 20080 San Sebastián, Spain

[§] Instituto Investigaciones Químicas (CSIC-US) and Centro de Innovación en Química Avanzada (ORFEO-CINQA) C/ Américo Vespucio 49, 41092 Sevilla, Spain, E-mail: jmlassa@iiq.csic.es

ABSTRACT: The Au^I-catalyzed reaction between terminal alkynes and aromatic haloalkynes proceeds through divergent pathways depending on the nature of the catalyst counteranion. Thus, cationic complexes containing strongly basic NHC ligands and non-coordinating anions such as BARF₄ catalyze the *cis* haloalkynylation of the terminal alkyne, whereas the introduction of a weakly basic triflate counteranion results in the stereoselective hydroalkynylation of the haloalkyne, yielding haloalkyne products in good yields and complete *trans* selectivity. Experimental and computational studies suggest that the hydroalkynylation reaction takes place via nucleophilic attack of the terminal alkyne to the C2 carbon of the activated haloalkyne, assisted by a concerted proton abstraction by the triflate, and that the protodeauration is the turnover limiting step, in agreement with an observed primary kinetic isotope effect.

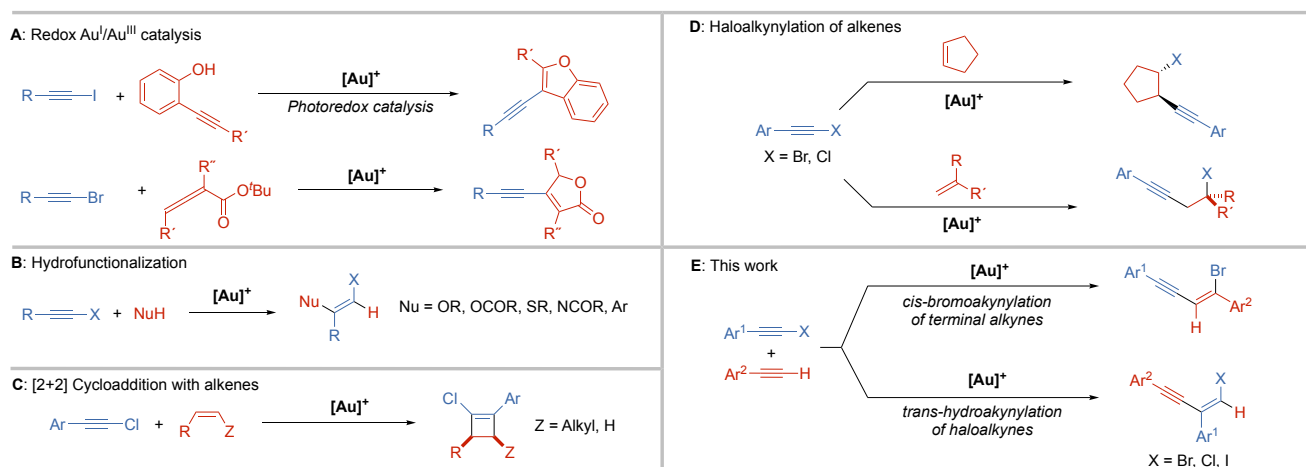
1. INTRODUCTION

Haloalkynes are recently gaining interest as versatile building blocks in synthetic organic chemistry.¹ Traditionally, these reagents have been used as a source of acetylides via metal-halogen exchange. However, with the development of transition metal catalysis, the number of transformations in which haloalkynes are used as reaction partners has increased exponentially.² Among them, amino-,^{3,4} oxy-,⁴ and carboalkynylation⁵ of olefins are useful transformations for the synthesis of a variety of functionalized alkynes, while the direct C–H alkynylation and inverse Sonogashira coupling are valuable alternatives for the selective introduction of alkynyl groups.⁶

Particular mention is deserved to processes enabled by Au^I catalysis. For instance, challenging catalytic transformations based on the redox

Au^I/Au^{III} couple have been recently applied to haloalkynes in the absence of external oxidants (Scheme 1A).⁷ Much effort has focused also in transformations in which the halogen atom is retained in the final product. Thus, the hydrofunctionalization of haloalkynes⁸ constitutes an important transformation leading to vinyl halides (Scheme 1B), versatile intermediates in organic synthesis and materials science. In particular, Au^I catalysis has been used to promote selective addition of O–H,⁹ S–H,¹⁰ N–H,¹¹ and X–H¹² bonds to haloalkynes, but examples of the hydrocarbofunctionalization (C–H addition) are rare: there are two recent reports on the Au-catalyzed hydroarylation of chloroalkynes^{9,13} and a few reports on intramolecular transformations¹⁴ but, to the best of our knowledge, there are no previous reports on the hydroalkynylation of haloalkynes.

Scheme 1. Au^I-catalyzed transformation of haloalkynes.

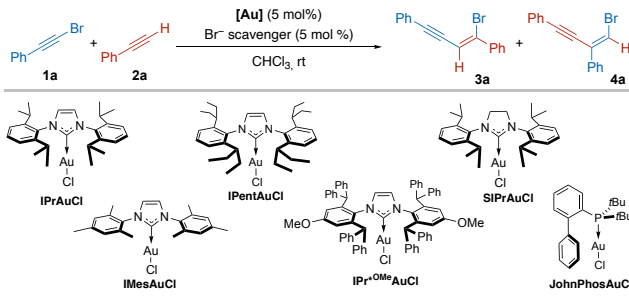


Recently, Zhang and co-workers reported on the intermolecular [2+2] cycloaddition between alkenes and chloroalkynes to afford chlorocyclobutenes¹⁵ (Scheme 1C). However, we¹⁶ and others,¹⁷ found later that subtle differences in the catalyst structure and reaction conditions allow to perform haloalkynylation reactions with the same alkene substrates (Scheme 1D). In this context, we decided to explore the cross reactivity of haloalkynes with alkynes. We now report on the discovery of catalysts-controlled divergent reaction pathways between haloalkynes and terminal alkynes, resulting in the bromoalkynylation on the terminal alkynes^{18,19} or the hydroalkynylation of the haloalkyne (Scheme 1E). These are challenging transformations considering that homodimerization of either chloroacetylenes²⁰ or terminal alkynes²¹ are potential side reactions that are known to be catalyzed by cationic Au^I complexes.

2. RESULTS AND DISCUSSION

Reaction Optimization. The reaction of (bromoethynyl)benzene **1a** with phenylacetylene **2a** was chosen as model for preliminary studies (Table 1). A first experiment was carried out with 5 mol% of IPrAuCl and 5 mol% of NaBAR^F₄ (sodium tetrakis[3,5-bis(trifluoromethyl)phenyl]borate) in CHCl₃ at room temperature. Under these conditions, the *cis* bromoalkynylation product **3a** was exclusively obtained although in a moderate yield (entry 1). Noteworthy, the nature of the halide scavenger has a marked effect in the selectivity of the reaction. For example, use of AgSbF₆ led also to the formation of **3a** as the main product, but a minor amount of isomer **4a**, identified as the *trans* hydroalkynylation product of the bromoalkyne **1a**, was also observed (entry 2). On the other hand, the use of AgNTf₂ also led to a **3a**:**4a** mixture, although the latter was isolated as the major component (entry 3). Fortunately, the reaction performed with AgOTf led to the exclusive formation of **4a** in an encouraging 58% yield (entry 4). No products were observed in control experiments performed with silver salts AgOTf, AgSbF₆ and AgNTf₂, confirming that silver is catalytically inactive in the reaction. Moreover, the preformed IPrAuOTf catalyst provides a similar result as the combination IPrAuCl/AgOTf (entry 5). Further ligand screening was then performed using triflate as counteranion. Less bulky NHC ligands were unproductive in this transformation (See Supporting Information for details): remarkably, even IMesAuCl failed as precatalyst (entry 6), highlighting the need of an efficient steric protection for the reaction to take place. Only extremely bulky representatives such as IPentAuCl or IPr^{*OMe}AuCl led to significant amounts of the product **4a** (entries 7 and 8). The best results were observed using SIPrAuCl: under the previous conditions, **4a** was isolated in 72% yield, although yet contaminated with a minor amount of **3a** (entry 9). However, reducing the excess of the alkyne reagent to 1.5 equiv and increasing the scale to 1 mmol, resulted in an excellent 80% yield of the pure product **4a** (entry 10) in only 5 h at room temperature. When the same reaction was performed without exclusion of water the yield dropped to 73% (entry 11), suggesting that hydrolysis of the terminal alkyne (particularly facilitated by the triflate counteranion)²² or the bromoalkyne²³ may compete in some extent under these conditions. Reaction performed with this catalyst in combination with AgOTs resulted very low yield (entry 12), while the introduction of more basic counteranions, using AgOAc or AgTFA as scavengers, totally inhibited the reaction (entries 13, 14). Bulky phosphine ligands were also tested, but both reactivity and selectivity were disappointing. For example, the reaction performed using JohnPhosAuCl as the precatalyst led to a mixture 1:2 of **3a**:**4a** in only 18% yield (entry 15) after 9 days. Finally, the SIPr ligand in combination with NaBAR^F₄ afforded the bromoalkynylation product **3a** in 50% yield (entry 16).

Table 1. Au^I-catalyzed reaction of (bromoethynyl)benzene and phenylacetylene.^a

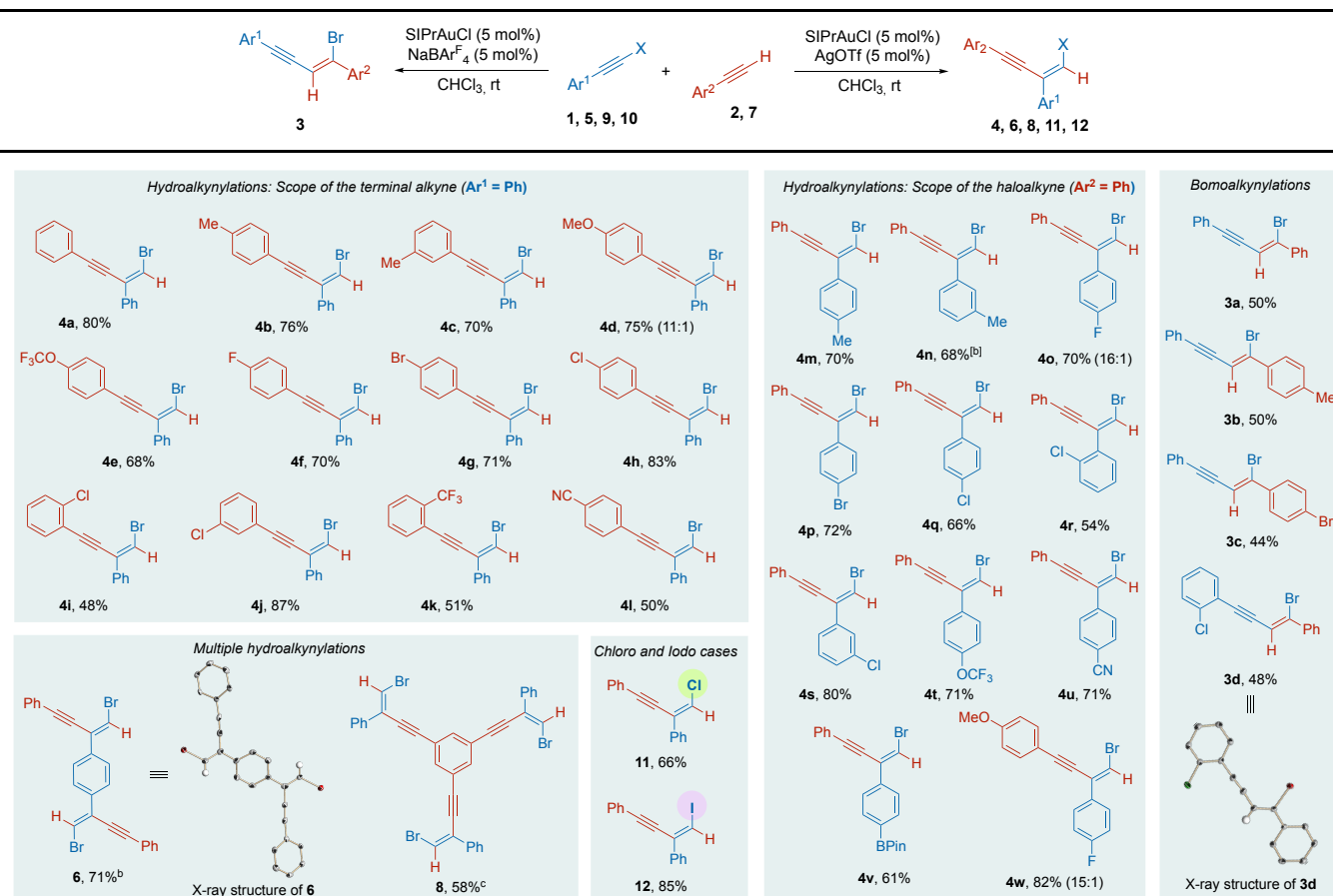


Entry	[Au]	Scavenger	Time (h)	3a : 4a	Yield (%) ^b
1	IPrAuCl	NaBAR ^F ₄	20	1:0	40
2	IPrAuCl	AgSbF ₆	15	6:1	52
3	IPrAuCl	AgNTf ₂	5	1:3.5	63
4	IPrAuCl	AgOTf	5	0:1	58
5	IPrAuOTf	-	5	0:1	51
6 ^c	IMesAuCl	AgOTf	120	--	--
7 ^c	IPentAuCl	AgOTf	5	1:9	62
8 ^c	IPr ^{*OMe} AuCl	AgOTf	24	1: 3.8	50
9	SIPrAuCl	AgOTf	5	1:14	72
10 ^{c,d}	SIPrAuCl	AgOTf	5	0:1	80
11 ^{c,d,e}	SIPrAuCl	AgOTf	5	0:1	73
12	SIPrAuCl	AgOTs	24	0:1	22
13	SIPrAuCl	AgOAc	72	--	--
14	SIPrAuCl	AgTFA	72	--	--
15 ^c	JohnPhosAuCl	AgOTf	216	1:2	18
16 ^c	SIPrAuCl	NaBAR ^F ₄	5	1:0	50

^a Reactions performed at 0.2 mmol scale in dry CHCl₃ (0.4 mL) at rt; **1a**:**2a** in a 1:3 ratio. Controlled by GC-MS. ^b Combined yields of isolated products. ^c **1a**:**2a** in a 1:1.5 ratio. ^d 1 mmol scale. ^e Reaction performed under aerobic conditions without exclusion of water.

Reaction Scope. With optimal conditions in hand, the reaction could be extended to a variety of aromatic bromoalkynes **1** and aryl acetylenes **2** with different substitution patterns (Table 2). To our delight, good to excellent selectivity towards hydroalkynylation products **4** was observed using both electron-withdrawing or donating groups on the aromatic ring of aryl acetylenes (compounds **4b-4l**), on the aromatic ring of the bromoalkynes (compounds **4m-4v**) or both (compound **4w**). Substitutions in *ortho*-, *meta*- or *para*- positions were also tolerated, although *ortho* substituents led to lower yields (**4i**, **4k** and **4r**). NOE experiments with compounds **4d**, **4g**, **4m** and **4p** demonstrated the formation of *trans*-hydroalkynylation products. The hydroalkynylation reaction could also be achieved using di- or tri-alkynyl-substituted benzenes. For example, reaction of 1,4-bis(bromoethynyl)benzene **5** using an excess of phenylacetylene **2a** led to the corresponding 1,4-bis[(*Z*)-1-bromo-4-

Table 2. Au^I-catalyzed hydroalkynylation of aromatic bromoalkynes and bromoalkynylation of terminal alkynes.^a



^a General reaction conditions for hydroalkynylation: haloalkyne (0.6 mmol), arylacetylene (0.9 mmol), CHCl_3 (1.2 mL). Isolated yields with > 20:1 ratio of 4:3 are reported, unless otherwise stated (in brackets). General reaction conditions for bromoalkynylation: bromoalkyne **1** (0.2 mmol), arylacetylene **2** (0.3 mmol), dry CHCl_3 (0.4 mL). Isolated yields. ^b **5** (0.6 mmol), **2a** (1.8 mmol), CHCl_3 (1.2 mL), SIPrAuCl (12 mol%), AgOTf (12 mmol%). ^c **7** (0.2 mmol), **1a** (1.2 mmol), CHCl_3 (1.2 mL), SIPrAuCl (15 mol%), AgOTf (15 mol%).

phenylbut-1-en-3-yn-2-yl]benzene **6** in an excellent 71% yield. Slow diffusion of hexane into a solution of the latter in diethyl ether afforded crystals suitable for single-crystal X-ray diffraction analysis, which confirmed unambiguously the assigned regio and stereoselectivity. The reaction works also using (bromoethynyl)benzene **1a** and 1,3,5-triethynylbenzene **7** as the arylacetylene substrate, leading to the corresponding tribromide adduct **8** in a satisfactory 58% yield.

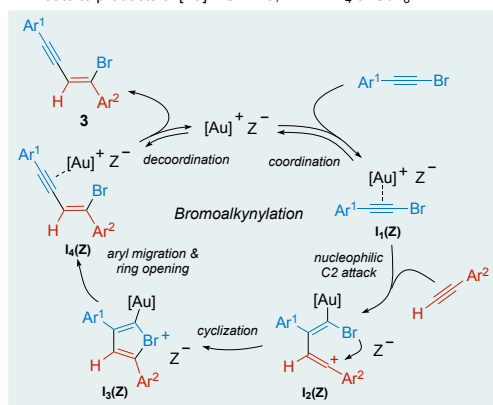
Importantly, (chloroethynyl)benzene **9** and (iodoethynyl)benzene **10** are also suitable substrates. Excellent selectivity towards hydroalkynylation products **11** and **12** was observed in both cases in their reactions with phenylacetylene **1a**, although a better yield was obtained in the reaction performed with iodoalkyne **10** (85% vs 66% yield). Finally, reactions performed with a selection of aromatic bromoalkynes **1** and aryl acetylenes **2** using $\text{SIPrAuCl}/\text{NaBAR}^{\text{F}_4}$ as catalytic system led exclusively to bromoalkynylation products **3** although with only moderate yields. X-Ray diffraction analysis of **3d** unambiguously confirmed the assigned regio and stereoselectivity.

Mechanisms. The critical counteranion effect²⁴ in the reactivity could be explained assuming the reaction mechanisms²⁵ depicted in Scheme 2. Thus, for the strongly acidic $\text{SIPrAu}^+\text{BAR}^{\text{F}_4-}$ catalyst, we assume that the reaction proceeds preferentially through attack of the alkyne to the C2 atom of the activated haloalkyne **I₁(Z)** (mechanism **A**). The resulting vinyl cation intermediate **I₂(Z)**²⁶ is then transformed into a cyclic, five-membered bromonium intermediate **I₃(Z)** which, upon 1,2-aryl migration with concomitant ring reopening provides the

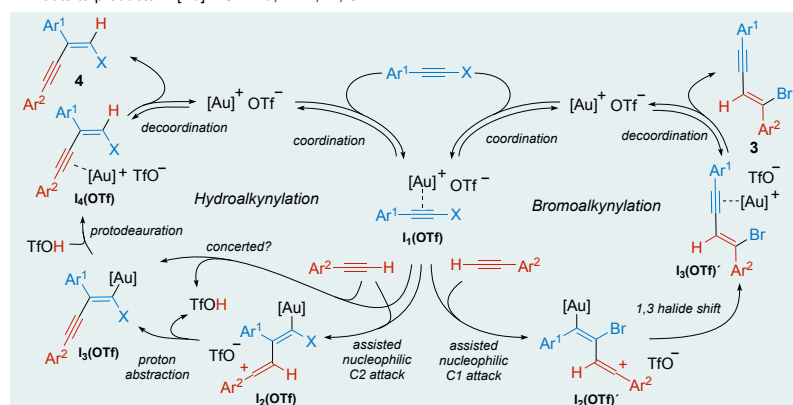
Au^{I} complex of the product **I₄(Z)**. This mechanism is strongly supported by ¹⁴C isotope labelling experiments that were first performed by Echavarren and co-workers^{17a} in a related context and, very recently, by Haberhauer and co-workers in the chloroalkynylation of internal alkynes.¹⁹ In the presence of a more basic counteranion, however, we hypothesized that deprotonation of the acidic H atom of the terminal alkyne at some point in the catalytic cycle could play a key role in the reaction outcome. Thus, the observed regioselectivity points again to a preferential attack at the C2 carbon of the activated haloalkyne **I₁(OTf)** to generate a strongly electrophilic vinyl cation intermediate **I₂(OTf)** that could be then deprotonated to afford the enyne complex **I₃(OTf)**. A final protodeauration step releases the product via **I₄(OTf)** and regenerates the cationic catalyst (mechanism **B**). Alternatively, the enyne complex **I₃(OTf)** could be formed directly from the activated haloalkyne **I₁(OTf)** by concerted C–C bond forming and C–H cleavage events, thereby avoiding the intermediacy of high-energy vinyl cation intermediates. The absence of reactivity with more basic OAc or TFA counteranions could be caused by a unfavourable $\text{SIPrAuZ} \rightleftharpoons \text{SIPrAu}(\text{haloalkyne})^+\text{Z}^-$ ($\text{Z} = \text{OAc}, \text{TFA}$) equilibrium, failing to provide a critical concentration of the activated substrate. The minor amounts of products **3** observed in some cases can be explained by cyclization of **I₂(OTf)** as in mechanism **A** or, after alternative attack at the C1 carbon, by formation of the vinyl cation **I₂(OTf)'** and subsequent 1,3-bromide shift to yield the product complex **I₃(OTf)'**.

Scheme 2. Proposed mechanisms for the divergent Au^I catalyzed reaction between haloalkynes and terminal alkynes.

A: Route to products **3**. [Au] = SIPrAu, Z = BAR^F₄ or SbF₆

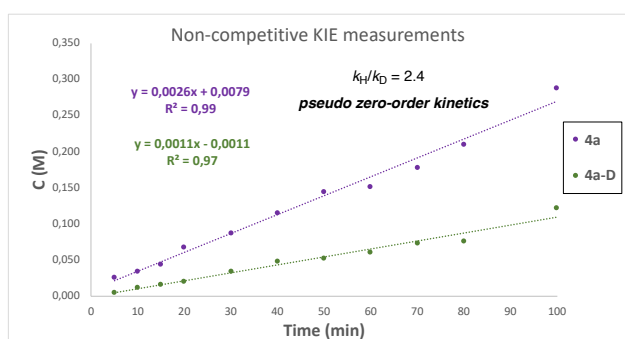
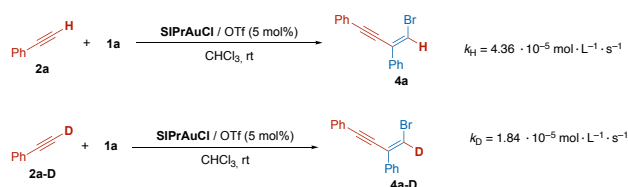


B: Route to products **4**. [Au] = SIPrAu, X = I, Br, Cl



Deuterium labelling and isotope effects. Mechanism **A** does not involve C–H bond breaking/forming events (not even the protodeauration commonly intervening in gold-catalyzed transformations) and, consequently, kinetic isotope effects (KIE) with deuterium-labeled reagents are not likely to be observed. In mechanism **B**, on the contrary, valuable information could be obtained from such experiments. In fact, intermolecular KIE was determined from the absolute rates of two parallel reactions of **1a** with **2a** and monodeuterated **2a-D** (Scheme 3). A primary KIE ($k_{\text{H}}/k_{\text{D}} = 2.4$) was measured in the hydroalkynylation reaction using SIPrAuCl/AgOTf as the catalyst under the optimized conditions. This result excludes C–C bond formation as the turnover-limiting step in a stepwise mechanism via **I₂(OTf)**, which is formed without any C–H/D bond cleavage or formation. Moreover, the observed zero-order kinetics in both reactions indicate that **I₃(OTf)** must be the resting state in the catalytic cycle²⁷ and that, therefore, protodeauration is the turnover limiting step.

Scheme 3. Kinetics and KIE determination for the hydroalkynylation reaction.

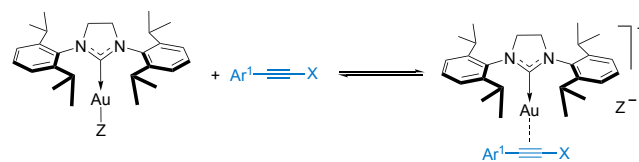


Additional experimental evidences point also to protodeauration as the turnover limiting step: First, the reaction slows down markedly in wet solvents, and it is known that water solvation of the acid increases the barrier of the protodeauration step.²⁸ Second, the reaction is facilitated by strong σ -donor ligands, which is again a characteristic of reactions featuring protodeauration as the turnover limiting step.^{28,29}

Computational Studies. Theoretical calculations have been carried out in order to validate the mechanistic hypothesis and rationalize the experimental observation.³⁰ The calculations were performed at the M06/def2tzvp//B3LYP/6-31G(d,p) (Au,SDD) (IEF-PCM, dichloromethane) level of theory, using the Gaussian 16 software. As model reaction we have chosen the Au^I-catalyzed reaction of (bromoethynyl)benzene **1a** with phenylacetylene **2a** employing SIPr-AuCl as precatalyst. With a non-basic anion (BAR^F₄), our calculations indicate a preference for the bromoalkynylation reaction pathway **A** to render the preferred product **3a**. The complete set of intermediates **I₁(Z)** and **I₄(Z)** and the corresponding transition states were calculated, and the results are in fair agreement with the experimental results and the calculations recently published for the chloroalkynylation of internal arylalkynes¹⁹ (see Supporting Information for details).

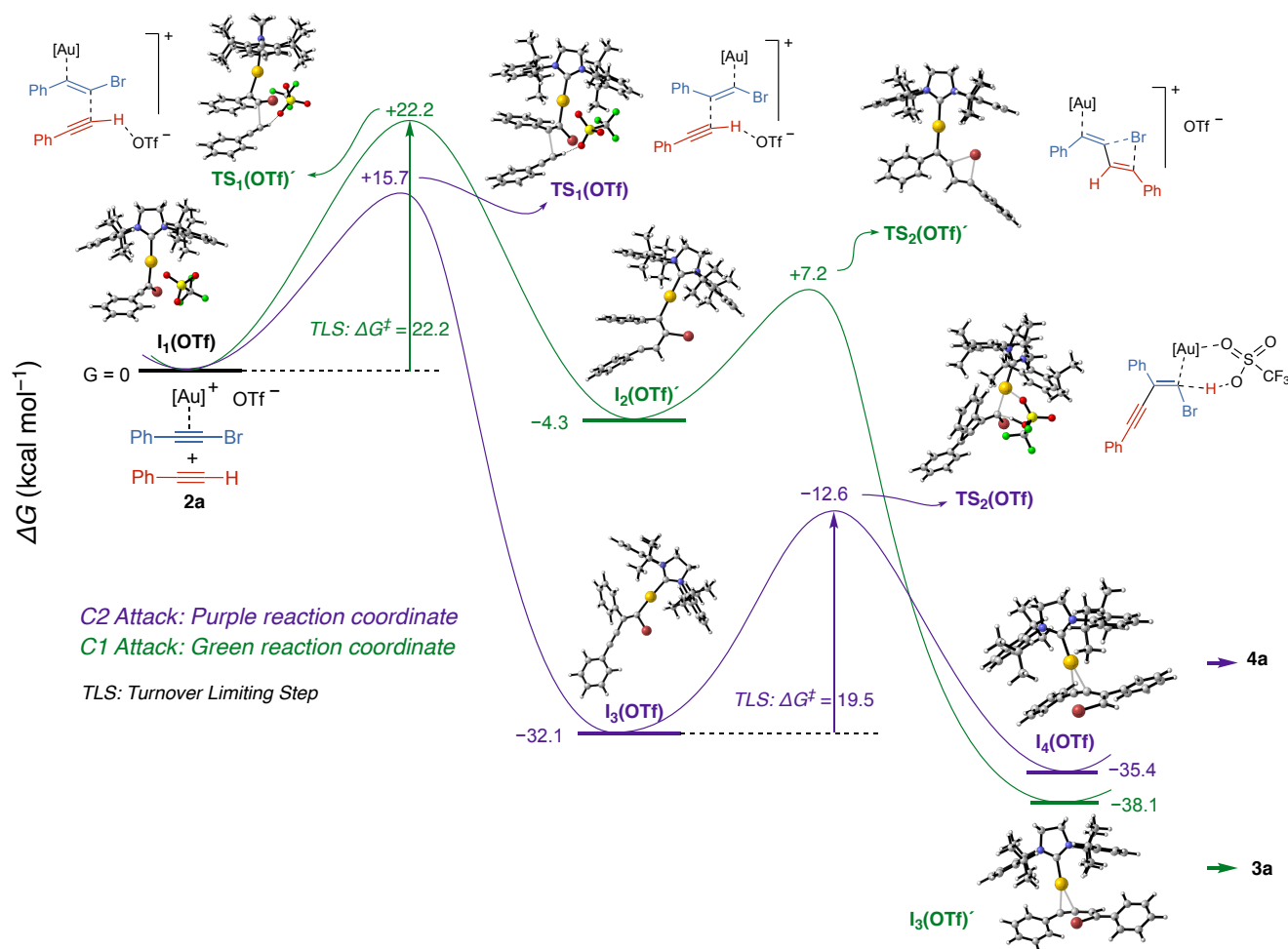
Regarding the hydroalkynylation mechanism **B**, we started by the analysis of the equilibrium energies for the ligand exchange (Scheme 4). In the case of weakly basic triflate, coordination of the bromoalkyne **2a** to form intermediate **I₁(OTf)** is exergonic by 18.1 kcal mol⁻¹, while the same process from catalysts with more basic TFA or OAc anions is endergonic by 22.5 and 29.9 kcal mol⁻¹, respectively.³¹ Such a difference can explain the lack of reactivity in these last cases, but there is an additional factor to take into consideration: the strength of acetic or trifluoroacetic acid could be not enough to efficiently promote the protodeauration.

Scheme 4. Computational analysis of the ligand exchange equilibrium.



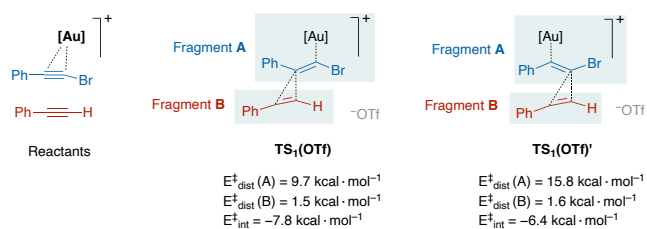
	Z	ΔG (kcal mol ⁻¹)	ΔE (kcal mol ⁻¹)
basicity ↓	OTf	-18.1	+9.4
	TFA	+22.5	+22.5
	OAc	+29.9	+30.5

Figure 1. Free energy profiles for the Au^I-catalyzed reactions of 1a and 2a using OTf as the counteranion.



With OTf as the counteranion, a different reaction pathway is preferred (Figure 1). The activation barrier for the initial C2 addition is lower (15.7 vs 16.5 kcal mol⁻¹ for OTf and BARF₄, respectively) but, in this case, the H-bonded transition state **TS₁(OTf)** (purple reaction coordinate) spontaneously deprotonates to render the neutral complex **I₃(OTf)** (+ TfOH) at -32.1 kcal mol⁻¹. Any attempts to locate the hypothetical vinyl cation intermediate [**I₂(OTf)** in Scheme 2] were unsuccessful, supporting preference for the concerted pathway. In agreement with all experimental evidences, the following protodeauration by triflic acid appears as the turnover limiting step with an activation energy of 19.5 kcal mol⁻¹ to yield the observed *trans* hydroalkynylation product **4a** (of bromoethynylbenzene) via intermediate **I₄(OTf)**. The alternative C1 attack was also calculated (green reaction coordinate). The nucleophilic attack has a higher activation energy [**TS₁(OTf)'** at 22.2 kcal mol⁻¹] and is the turnover limiting step. In this case, a vinyl cation intermediate **I₂(OTf)'** is located at G = -4.3 kcal mol⁻¹, yielding the bromoalkynylation product **3a** after a relatively fast 1,3 bromine shift [**TS₂(OTf)'** at +7.2 kcal mol⁻¹] and ensuing decooordination of the resulting intermediate **I₃(OTf)'**. The strong difference in energy between **TS₁(OTf)** and **TS₁(OTf)'** explains the preferential attack at C2, regularly observed in Au^I-catalyzed addition to haloalkynes. In order to better understand the origin of this energy difference, a distortion/interaction energy analysis³² of the C–C bond forming process was carried out by separating each transition state into two moieties (fragments **A** and **B**, Scheme 5). This analysis shows that fragment **B** gets only slightly distorted, and in a similar amount in both transition states (1.5 and 1.6 kcal mol⁻¹ respectively). On the contrary, fragment **A** suffers a larger

Scheme 5. Analysis of distortion/interaction energies for **TS₁(OTf)** and **TS₁(OTf)'**.



deformation, and there is a marked difference between both transition structures [9.7 vs 15.8 kcal mol⁻¹ for **TS₁(OTf)** and **TS₁(OTf)'**, respectively], as gold has to move from the terminal to the internal C atom of the triple bond. The stabilizing interaction energy is quite similar in both cases, slightly better in **TS₁(OTf)** than in **TS₁(OTf)'**, further favoring the C2 attack.

Together, these calculations support the starting hypothesis, explaining the preference for the C2 attack to the haloalkyne and explaining the observed counteranion effect. Moreover, the results are in agreement with the kinetic experiments that support protodeauration as the turnover limiting step.

CONCLUSIONS

In summary, two divergent reaction outcomes for the Au^I catalyzed cross reaction between terminal alkynes and haloalkynes can be

achieved just by modifying the counteranion of the catalytically active cationic species. While bromoalkynylation of the terminal alkyne is observed when $\text{SIPrAuCl}/\text{NaBAr}_4^+$ is used, an unprecedented hydroalkynylation of bromoalkynes can be selectively performed in high yield with a $\text{SIPrAuCl}/\text{AgOTf}$ catalytic system. The triflate counteranion serves in this last case a perfect proton shuttle, basic enough to assist a concerted C–C bond formation with simultaneous deprotonation, but still allowing a favorable exchange equilibrium to the activated haloalkyne. The computational results are in fair agreement with the observed reactivity and kinetic isotope effect.

ASSOCIATED CONTENT

Supporting Information

The Supporting Information is available free of charge on the ACS Publications website.

Experimental procedures, optimization studies, characterization data, and NMR spectra for new compounds (PDF).

Crystallographic data for **3d** (CIF)

Crystallographic data for **6** (CIF)

Detailed computational study. Calculated structures and energies (PDF)

Three-dimensional structural data of **SIPrAuOTf**

Three-dimensional structural data of **I₁(OTf)**

Three-dimensional structural data of **TS₁(OTf)**

Three-dimensional structural data of **I₃(OTf)**

Three-dimensional structural data of **TS₂(OTf)**

Three-dimensional structural data of **I₄(OTf)**

Three-dimensional structural data of **TS₁(OTf)**'

Three-dimensional structural data of **I₂(OTf)**'

Three-dimensional structural data of **TS₂(OTf)**'

Three-dimensional structural data of **I₃(OTf)**'

Three-dimensional structural data of **I₁(Z)**

Three-dimensional structural data of **TS₁(Z)**

Three-dimensional structural data of **I₂(Z)**

Three-dimensional structural data of **I₃(Z)**

Three-dimensional structural data of **TS₂(Z)**

Three-dimensional structural data of **I₄(Z)**

AUTHOR INFORMATION

Corresponding Authors

Elena Díez – Departamento de Química Orgánica, Universidad de Sevilla and Centro de Innovación en Química Avanzada (ORFEO–CINQA), Sevilla 41012, Spain; ORCID: 0000-0002-1899-8003. Email: ediez@us.es

Enrique Gómez-Bengoa – Departamento de Química Orgánica I, Universidad del País Vasco, UPV/EHU, Apdo. 1072, 20080 San Sebastián, Spain; ORCID: 0000-0002-8753-3760. Email: enrique.gomez@ehu.es

Rosario Fernández – Departamento de Química Orgánica, Universidad de Sevilla and Centro de Innovación en Química Avanzada (ORFEO–CINQA), Sevilla 41012, Spain; ORCID: 0000-0002-1755-1525. Email: rfernandez@us.es

José M. Lassaletta – Instituto de Investigaciones Químicas (CSIC-US) and Centro de Innovación en Química Avanzada (ORFEO–CINQA), Sevilla 41092, Spain; ORCID: 0000-0003-1772-2723. Email: jmlassa@iiq.csic.es

Authors

Pedro D. García-Fernández – Departamento de Química Orgánica, Universidad de Sevilla and Centro de Innovación en Química Avanzada (ORFEO–CINQA), Sevilla 41012, Spain; ORCID: 0000-0003-3078-9420.

Javier Iglesias-Sigüenza – Departamento de Química Orgánica, Universidad de Sevilla and Centro de Innovación en Química Avanzada (ORFEO–CINQA), Sevilla 41012, Spain; ORCID: 0000-0001-8846-2303.

Paula S. Rivero-Jerez – Departamento de Química Orgánica, Universidad de Sevilla and Centro de Innovación en Química Avanzada (ORFEO–CINQA), Sevilla 41012, Spain. ORCID: 0000-0003-2498-5564.

Present Addresses

[∇] Departamento de Química Orgánica, Facultad de Química y de Farmacia, Pontificia Universidad Católica de Chile, Av. Vicuña Mackenna 4860, Casilla 306, Correo 22, Santiago, Chile.

Notes

The authors declare no competing financial interests.

ACKNOWLEDGMENT

This work was supported by the Spanish MINECO (grants PID2019-106358GB-C21 and PID2019-106358GB-C22 and predoctoral fellowship to P. D. G.-F.), European FEDER funds and the Junta de Andalucía (Grants P18-FR-3531, P18-FR-644 and US-1262867). We also thank SGlker (UPV/EHU) for providing human and computational resources

REFERENCES

- (1) Wu, W.; Jiang, H. Haloalkynes: A powerful and versatile building block in organic synthesis. *Acc. Chem. Res.* **2014**, *47*, 2483–2504.
- (2)) Petko, D.; Koh, S.; Tam, W. Transition Metal-Catalyzed Reactions of Alkynyl Halides. *Curr. Org. Synth.* **2019**, *16*, 546–582.
- (3) Nicolai, S.; Piemontesi, C.; Waser, J. A Palladium-Catalyzed Aminoalkynylation Strategy towards Bicyclic Heterocycles: Synthesis of (±)-Trachelanthamidine. *Angew. Chem. Int. Ed.* **2011**, *50*, 4680–4683.
- (4) (a) Nicolai, S.; Waser, J. Pd(0)-Catalyzed Oxy- and Aminoalkynylation of Olefins for the Synthesis of Tetrahydrofurans and Pyrrolidines. *Org. Lett.* **2011**, *13*, 6324–6327. (b) Nicolai, S.; Sedigh-Zadeh, R.; Waser, J. Pd(0)-Catalyzed Alkene Oxy- and Aminoalkynylation with Aliphatic Bromoacetylenes. *J. Org. Chem.* **2013**, *78*, 3783–3801. (c) Sun, N.; Li, Y.; Yin, G.; Jiang, S. Palladium-Catalyzed Alkynylative Lactonization of Unsaturated Bicyclic Carboxylic Acids: Synthesis of Fused Polycyclic γ -Lactone Compounds. *Eur. J. Org. Chem.* **2013**, 2541–2544.
- (5) Nicolai, S.; Swallow, P.; Waser, J. Intramolecular palladium-catalyzed alkene carboalkynylation. *Eur. J. Org. Chem.* **2013**, 2541–2544.
- (6) Selected examples: (a) Tobisu, M.; Ano, Y.; Chatani, N. Palladium-Catalyzed Direct Alkynylation of C–H Bonds in Benzenes. *Org. Lett.* **2009**, *11*, 3250–3252. (b) Dudnik, A. S.; Gevorgyan, V. Formal Inverse Sonogashira Reaction: Direct Alkynylation of Arenes and Heterocycles with Alkynyl Halides. *Angew. Chem. Int. Ed.* **2010**, *49*, 2096–2098 (c) Tan, E.; Quinonero, O.; Elena de Orbe, M.; Echavarren, A. M. Broad-scope Rh-Catalyzed Inverse-Sonogashira Reaction Directed by Weakly Coordinating Groups. *ACS Catal.* **2018**, *8*, 2166–2172. (d) Mahato, S. K.; Chatani, N. The Iridium(III)-Catalyzed Direct C(sp²)– and C(sp³)–H Alkynylation of 2-Acylimidazoles with Various Alkynyl Bromides: Understanding the Full Catalytic Cycle. *ACS Catal.* **2020**, *10*, 5173–5178. (e) Porey, S.; Zhang, X.; Bhowmick, S.; Singh, V. K.; Guin, S.; Paton, R. S.; Maiti, M. Alkyne Linchpin Strategy for Drug: Pharmacophore Conjugation: Experimental and Computational Realization of a Meta-Selective Inverse Sonogashira Coupling. *J. Am. Chem. Soc.* **2020**, *142*, 3762–3774. (f) Tan, E.; Zanini, M.; Echavarren, A. M. Iridium-Catalyzed β -Alkynylation of Aliphatic Oximes as Masked Carbonyl Compounds and Alcohols. *Angew. Chem. Int. Ed.* **2020**, *59*, 10470–10473.
- (7) (a) Xia, Z.; Corcé, V.; Zhao, F.; Przybylski, C.; Espagne, A.; Jullien, L.; Le Saux, T.; Gimbert, Y.; Dossmann, H.; Mouriès-Mansuy, V.; Ollivier, C.; Fensterbank, L. Photosensitized oxidative addition to gold(I) enables alkynylative cyclization of o-alkynylphenols with iodoalkynes. *Nat. Chem.* **2019**, *11*, 797–805. (b) Yang, Y.; Schiebl, J.; Zallouz, S.; Göker, V.; Gross, J.; Rudolph, M.; Rominger, F.; Hashmi, A. S. K. Gold-Catalyzed C(sp²)–C(sp) Coupling by Alkynylation through Oxidative Addition of Bromoalkynes. *Chem. Eur. J.* **2019**, *25*, 9624–9628.

- (8) Recent review: Cadierno, V. Metal-catalyzed hydrofunctionalization reactions of haloalkynes. *Eur. J. Inorg. Chem.* **2020**, 886–898.
- (9) Liu, C.; Xue, Y.; Ding, L.; Zhang, H.; Yang, F. Au-Catalyzed addition of nucleophiles to chloroalkynes: A regio- and stereoselective synthesis of (Z)-alkenyl chlorides. *Eur. J. Org. Chem.* **2018**, 6537–6540.
- (10) Zeng, X.; Chen, B.; Lu, Z.; Hammond, G. B.; Xu, B. Homogeneous and Nanoparticle Gold-Catalyzed Hydrothiocyanation of Haloalkynes. *Org. Lett.* **2019**, 21, 2772–2776.
- (11) Liu, C.; Yang, F. Au-Catalyzed Stereoselective Ritter Reaction of Haloalkynes with Nitriles for (Z)- β -Halogenated Enamides. *Eur. J. Org. Chem.* **2019**, 6867–6870.
- (12) Zeng, X.; Liu, S.; Hammond, G. B.; Xu, B. Hydrogen-bonding-assisted Brønsted acid and Gold catalysis: Access to both (E)- and (Z)-1,2-haloalkenes via hydrochlorination of haloalkynes. *ACS Catal.* **2018**, 8, 904–909.
- (13) Adak, T.; Schulmeister, J.; Dietl, M. C.; Rudolph, M.; Rominger, F.; Hashmi, A. S. K. Gold-Catalyzed Highly Chemo- and Regioselective C-H Bond Functionalization of Phenols with Haloalkynes. *Eur. J. Org. Chem.* **2019**, 3867–3876.
- (14) Selected examples (a) Staben, S. T.; Kennedy-Smith, J. J.; Toste, F. D. Gold(I)-Catalyzed 5-endo-dig Carbocyclization of Acetylenic Dicarboxyl Compounds. *Angew. Chem. Int. Ed.* **2004**, 43, 5350–5352. (b) Mamane, V.; Hannen, P.; Fürstner, A. Synthesis of Phenanthrenes and Polycyclic Heteroarenes by Transition-Metal Catalyzed Cycloisomerization Reactions. *Chem. Eur. J.* **2004**, 10, 4556–4575. (c) Morán-Poladura, P.; Rubio, E.; González, J. M. Intramolecular C–H Activation through Gold(I)-Catalyzed Reaction of Iodoalkynes. *Angew. Chem. Int. Ed.* **2015**, 54, 3052–3055. (d) Rong, Z.; Echavarren, A. M. Broad scope gold(I)-catalyzed polyenyne cyclisations for the formation of up to four carbon-carbon bonds. *Org. Biomol. Chem.* **2017**, 15, 2163–2167. (e) Speck, K.; Karaghiosoff, K.; Magauer, T. Sequential O–H/C–H Bond Insertion of Phenols Initiated by the Gold(I)-Catalyzed Cyclization of 1-Bromo-1,5-enynes. *Org. Lett.* **2015**, 17, 1982–1985.
- (15) Bai, Y.-B.; Luo, Z.; Wang, Y.; Gao, J.-M.; Zhang, L. Au-Catalyzed intermolecular [2+2] cycloadditions between chloroalkynes and unactivated alkenes. *J. Am. Chem. Soc.* **2018**, 140, 5860–5865.
- (16) García-Fernández, P. D.; Izquierdo, C.; Iglesias-Sigüenza, J.; Díez, E.; Fernández, R.; Lassaletta, J. M. Au(I)-Catalyzed Haloalkynylation of Alkenes. *Chem. Eur. J.* **2020**, 26, 629–633.
- (17) (a) De Orbe, M. E.; Zanini, M.; Quinero, O.; Echavarren, A. Gold- or Indium-Catalyzed Cross-Coupling of Bromoalkynes with Allylsilanes through a Concealed Rearrangement. *ACS Catal.* **2019**, 9, 7817–7822. (b) Kreuzahler, M.; Haberhauer, G. Gold(I)-catalyzed chloroalkynylation of 1,1-disubstituted alkenes via 1,3-chlorine shift: A combined experimental and theoretical study. *J. Org. Chem.* **2019**, 84, 8210–8224.
- (18) For a Pd-catalyzed bromoalkynylation of internal alkynes see: Li, Y.; Liu, X.; Jiang, H.; Feng, Z. Expedient synthesis of functionalized conjugated enynes: Palladium-catalyzed bromoalkynylation of alkynes. *Angew. Chem. Int. Ed.* **2010**, 49, 3338–3341.
- (19) During the preparation of this manuscript, the group of Haberhauer published experimental and computational studies on the chloroalkynylation of internal alkynes: (a) Kreuzahler, M.; Haberhauer, G. Gold(I)-catalyzed haloalkynylation of aryl alkynes: Two pathways, one goal. *Angew. Chem. Int. Ed.* **2020**, 59, 9433–9437. (b) Kreuzahler, M.; Haberhauer, G. Cyclopropenylmethyl Cation – A Concealed Intermediate in Gold(I)-Catalyzed Reactions. *Angew. Chem. Int. Ed.* 10.1002/anie.202006245
- (20) Kreuzahler, M.; Daniels, A.; Wolper, C.; Haberhauer, G. 1,3-Chlorine Shift to a Vinyl Cation: A Combined Experimental and Theoretical Investigation of the E-Selective Gold(I)-Catalyzed Dimerization of Chloroacetylenes. *J. Am. Chem. Soc.* **2019**, 141, 1337–1348.
- (21) Sun, S.; Kroll, J.; Luo, Y.; Zhang, L. Gold-Catalyzed Regioselective Dimerization of Aliphatic Terminal Alkynes. *Synlett* **2012**, 23, 54–56.
- (22) Ebule, R. E.; Malhotra, D.; Hammond, G. B.; Xu, B. Ligand Effects in the Gold Catalyzed Hydration of Alkynes. *Adv. Synth. Catal.* **2016**, 358, 1478–1481.
- (23) Xie, L.; Wu, Y.; Yi, W.; Zhu, L.; Xiang, J.; He, W. Gold-Catalyzed Hydration of Haloalkynes to α -Halomethyl Ketones. *J. Org. Chem.* **2013**, 78, 9190–9195.
- (24) (a) Rocchigiani, L.; Jia, M.; Bandini, M.; Macchioni, A. Assessing the Role of Counterion in Gold-Catalyzed Dearomatization of Indoles with Allenamides by NMR Studies. *ACS Catal.* **2015**, 5, 3911–3915. (b) Gatto, M.; Belanzoni, P.; Belpassi, L.; Biasiolo, L.; Del Zotto, A.; Tarantelli, F.; Zuccaccia, D. Solvent-, Silver-, and Acid-Free NHC-Au-X Catalyzed Hydration of Alkynes. The Pivotal Role of the Counterion. *ACS Catal.* **2016**, 6, 7363–7376. (c) Schießl, J.; Schulmeister, J.; Doppiu, A.; Wörner, E.; Rudolph, M.; Karch, R.; Hashmi, A. S. K. An Industrial Perspective on Counter Anions in Gold Catalysis: On Alternative Counter Anions. *Adv. Synth. Catal.* **2018**, 360, 3949–3959. (d) Schießl, J.; Schulmeister, J.; Doppiu, A.; Wörner, E.; Rudolph, M.; Karch, R.; Hashmi, A. S. K. An Industrial Perspective on Counter Anions in Gold Catalysis: Underestimated with Respect to “Ligand Effects” *Adv. Synth. Catal.* **2018**, 360, 2493–2502.
- (25) (a) Hashmi, A. S. K. Homogeneous Gold Catalysis Beyond Assumptions and Proposals—Characterized Intermediates. *Angew. Chem. Int. Ed.* **2010**, 49, 5232–5241. (b) Greisch, J.-F.; Weis, P.; Brendle, K.; Kappes, M. M.; Haler, J. R. N.; Far, J.; De Pauw, E.; Albers, C.; Bay, S.; Wurm, T.; Rudolph, M.; Schulmeister, J.; Hashmi, A. S. K. Detection of Intermediates in Dual Gold Catalysis Using High-Resolution Ion Mobility Mass Spectrometry. *Organometallics* **2018**, 37, 1493–1500. (c) Lauterbach, T.; Asiri, A. M.; Hashmi, A. S. K. Organometallic Intermediates of Gold Catalysis. *Adv. Organomet. Chem.* **2014**, 62, 261–297.
- (26) For the access to such vinyl cations by electrophilic attack to arylalkynes in gold catalysis, see: (a) Wurm, T.; Bucher, J.; Duckworth, S. B.; Rudolph, M.; Rominger, F.; Hashmi, A. S. K. On the Gold-Catalyzed Generation of Vinyl Cations from 1,5-Diynes. *Angew. Chem. Int. Ed.* **2017**, 56, 3364–3368. (b) Weingand, V.; Wurm, T.; Vethacke, V.; Dietl, M. C.; Ehjeij, D.; Rudolph, M.; Rominger, F.; Xie, J.; Hashmi, A. S. K. Intermolecular Desymmetrizing Gold-Catalyzed Yne-Yne Reaction of Push–Pull Diarylalkynes. *Chem. Eur. J.* **2018**, 24, 3725–3728. (c) Tavakkolifard, S.; Sekine, K.; Reichert, L.; Ebrahimi, M.; Museridz, K.; Michel, E.; Rominger, F.; Babaahmadi, R.; Ariafard, A.; Yates, B. F.; Rudolph, M.; Hashmi, A. S. K. Gold-Catalyzed Regiospecific Annulation of Unsymmetrically Substituted 1,5-Diynes for the Precise Synthesis of Bispentalenes. *Chem. Eur. J.* **2019**, 25, 12180–12186. (d) Claus, V.; Schukin, M.; Harrer, S.; Rudolph, M.; Rominger, F.; Asiri, A. M.; Xie, J.; Hashmi, A. S. K. Gold-Catalyzed Dimerization of Diarylalkynes: Direct Access to Azulenes. *Angew. Chem. Int. Ed.* **2018**, 57, 12966–12970.
- (27) Blackmond, D. G. Kinetic Profiling of Catalytic Organic Reactions as a Mechanistic Tool. *J. Am. Chem. Soc.* **2015**, 137, 10852–10866.
- (28) Babaahmadi, R.; Ghanbari, P.; Rajabi, N. A.; Hashmi, A. S. K.; Yates, B. F.; Ariafard, A. A theoretical study on the protodeauration step of the gold(I)-catalyzed organic reactions. *Organometallics* **2015**, 34, 3186–3195.
- (29) Wang, W.; Hammond, G. B.; Xu, B. Ligand effects and ligand design in homogeneous Gold(I) catalysis. *J. Am. Chem. Soc.* **2012**, 134, 5697–5705.
- (30) Reviews: (a) Faza, O. N.; López, C. S. Computational Approaches to Homogeneous Gold Catalysis. *Top. Curr. Chem.* **2015**, 357, 213–283. (b) Pyykkö, P. Theoretical chemistry of gold. III. *Chem. Soc. Rev.* **2008**, 37, 1967–1997.
- (31) Apparently, the computed thermal correction to Gibbs energy might suffer from some inconsistencies in the case of the triflate anion, affording a distorted ΔG of -18.1 kcal mol $^{-1}$. A more logical value is obtained using the electronic energy ΔE , which still supports a strong reactivity difference between the three anions. Similar results were obtained with alternative computational methods (see the Supporting Information for details).
- (32) (a) Jin, R.; Liu, S.; Lan, Y. Distortion–interaction analysis along the reaction pathway to reveal the reactivity of the Alder-ene reaction of enes. *RSC Adv.* **2015**, 5, 61426–61435. (b) Bickelhaupt, F. M.; Houk, K. N. Analyzing Reaction Rates with the Distortion/Interaction-Activation Strain Model. *Angew. Chem. Int. Ed.* **2017**, 56, 10070–10086.

